

## STRUCTURAL, THERMAL AND RHEOLOGICAL STUDIES OF VIRGIN COCONUT OIL-BASED LAMELLAR LIQUID CRYSTALS FROM MIXED TWEEN 85 AND TWEEN 65

Norzakiatul Husna Isnolamran<sup>1</sup>, Wan Rusmawati Wan Mahamod<sup>1\*</sup>, Norlaili Abu Bakar<sup>1</sup>, Norhayati Hashim<sup>1</sup>, Nor Ain and Siti Aisyah Shamsudin<sup>2</sup>

<sup>1</sup>Department of Chemistry, Faculty of Science and Mathematics, Universiti Pendidikan Sultan Idris, 35900 Tanjong Malim, Perak, Malaysia.

<sup>2</sup>Department of Applied Physics, Faculty of Science and Technology, Universiti Kebangsaan Malaysia, 43600 Bangi, Selangor, Malaysia.

\*[rusmawati@fsmf.upsi.edu.my](mailto:rusmawati@fsmf.upsi.edu.my)

---

**Abstract.** The uniqueness and diversity of the liquid crystal structure have attracted many of scholars of pharmaceutical and cosmetic products to conduct intensive studies on the structure of this emulsion. In this study, virgin coconut oil (VCO)-based lamellar liquid crystal (VL $\alpha$ ) from mixed tween 85 and tween 65 was synthesized via titration method. The structural, thermal and rheological studies were performed using polarized light microscope (PLM) and small angle x-ray scattering (SAXS), differential scanning calorimetry (DSC) and rheometer, respectively. The effect of VCO content and the addition of crisaborole (CB) on the entire characterization were also carried out. The maltose cross and oily textures that appear in the PLM micrographs and the SAXS spectrum confirms the presence of a lamellar phase (L $\alpha$ ) in the system. This L $\alpha$  sample is thermally stable and pseudoplastic in nature with shear thinning behaviour. The VCO content was discovered to affect the lamellar texture and the rheological profile without having a substantial impact on thermal stability. Meanwhile the presence of CB did not cause considerable disturbance to the lamellar structure. This synthesized lamellar phase accompanied by VCO as a value-added material has its own distinctive rheological behaviour, promising wide application potential such as topical application.

**Keyword:** VCO-based lamellar liquid crystal, SAXS, DSC and rheological properties.

---

### Article Info

Received 10<sup>th</sup> October 2021

Accepted 28<sup>th</sup> February 2022

Published 20<sup>th</sup> April 2022

Copyright Malaysian Journal of Microscopy (2022). All rights reserved.

ISSN: 1823-7010, eISSN: 2600-7444

## Introduction

Lamellar liquid crystals ( $L\alpha$ ) consist of oily phase and water phase separated by ordered surfactant molecules that protrude into the intervening layers of aqueous interface [1]. The unique characteristics of liquid crystals promote a great potential for innovative applications in the pharmaceutical field due to their similarity with the stratum corneum lipid structure of the living organism [2]. Moreover, the  $L\alpha$  system can be used as a drug or nutrient carrier in pharmaceuticals and cosmetics due to its capacity to control and sustain drug release [3].

Virgin coconut oil (VCO) is an oil produced organically from the mature kernel of the coconut fruit using various natural and mechanical methods. The high concentration of lauric acid and lactic acid bacteria in VCO has been shown to have antibacterial properties capable of killing pathogenic bacteria [4]. Other biological actions examined from VCO include anticancer, antibacterial, analgesic, antipyretic, and anti-inflammatory properties. VCO was often used to moisturize and cure skin problems. The emollient qualities of VCO have previously been effectively evaluated on atopic dermatitis patients, demonstrating VCO capabilities as a novel natural emollient to be used in xerosis therapy [5].

Crisaborole (CB) is a nonsteroidal, topical, anti-inflammatory phosphodiesterase (PDE-4) inhibitor and cytokine release inhibitor that has been studied in biochemical, cell-based, and animal studies for the treatment of mild to moderate atopic dermatitis (AD). AD is a chronic skin condition characterized by severe pruritus, skin barrier dysfunction, and eczematous lesions that necessitates aggressive therapy. Thus, CB is now being suggested since it has positive results. The boron component enables the synthesis of low molecular weight compounds, allowing penetration through the dermis layer [6].

A good biocompatibility surfactant is needed to construct  $L\alpha$  systems in line with to meet required application. In this study, Tween 65, polyoxyethylene (20) sorbitantristearate (T65), with HLB value of 10.5 and Tween 85, polyoxyethylene (20) sorbitan trioleate (T85) with HLB value of 11 has been used. T65 and T85 are pharmaceutically accepted non-toxic surfactant that has been currently used in a field of pharmaceutical, cosmetic formulation and food emulsifier [7]. Internal factors such as the type of surfactant or co-surfactant, oil and water content, impact the phase transition, strength, and stability of  $L\alpha$  systems. Temperature, pH, pressure, magnetic field, and other external variables all regulate the liquid crystals production technique [8]. Additionally, the goal of this research is to explore the effect of oil contents and the presence of crisaborole (CB) on the thermal stability and rheological characteristics of  $VL\alpha$ . The polarized light microscope (PLM), small angle X-ray scattering (SAXS), differential scanning calorimetry (DSC), and rheometer were used to characterize and study the thermal and rheological profile of  $VL\alpha$  samples. This study is a first step toward a more thorough examination of the possibility of using CB-incorporated lamellar phases in the pharmaceutical, cosmetics, and microfluidics industries.

## Materials and methods

Refined virgin coconut oil was purchased from a local company. The oil was packed in a transparent, airtight plastic bottle and appeared to be colourless. Tween 65 (Polyoxyethylene (20) sorbitan tristearate) (T65), Tween 85 (Polyoxyethylene sorbitan Trioleate) (T85) and Crisaborole ( $C_{14}H_{10}BNO_3$ ) were purchased from Fluka and were used without further purification. Water used was double distilled and deionized.

**Preparation of lamellar liquid crystals.** Based on ternary diagrams generated by Dalila (2012) utilizing the titration technique with modification, VCO-based lamellar liquid crystals (VL $\alpha$ ) of the T85:T65/H<sub>2</sub>O/VCO system was prepared [9]. A sample composition at fixed T85 to T65 (mixed surfactant, Ms) ratio and a mixed surfactant to water (Ms/H<sub>2</sub>O) ratio of 9:1 and 0.69:0.31, respectively was chosen. Two concentrations of VCO (3.5% and 6%) were studied. Five grams of liquid crystal sample at selected weight composition was prepared using two steps at 25 °C. The first step was the preparation of aqueous solution containing of T85 and deionized water at the desired weight composition. The oil solution was prepared by firstly melted T65 in a water bath at 60 °C before being thoroughly mixed with VCO using vortex mixer. The aqueous solution was then gradually added to the oil solution while continuously mixing for 10 minutes at 4000 rpm before centrifugation to produce a homogeneous phase. The mixing and centrifugation processes were performed repeatedly until only the monolayer phase was obtained. Lastly, the anisotropy behaviour of the stable homogeneous lamellar phase was monitored under a polarizer film after being stored at room temperature for 24 hours to achieve equilibrium. CB was incorporated into VL $\alpha$  using the same method with a slight modification in which it was first dissolved in a VCO before being mixed with other components. The percentages of CB of 5% were used in the systems.

**Polarized light microscope.** The microscopic texture and phase transition of liquid crystals (LC) was observed under polarized light microscope (PLM) (Leica DM EP, Wetzlar, Germany). The images were captured using a Nikon H550S optical camera with an exposure controller attached to the microscope. The samples with a thickness of about  $\pm 13$   $\mu\text{m}$  were placed between the glass slides and coverslip. The light intensities were set at a minimum to prevent the samples from being damaged. The samples were observed at 5x, 10x and 20x magnification. The patterns of the VL $\alpha$  systems were examined.

**Small angle X-ray scattering.** SAXS is very effective in determining the molecular dimensions of LC and distinguishing phases with different topologies, as well as focusing on the internal structure of liquid crystalline systems and how drug and additive interactions are influenced because it can detect small angles ( $\theta < 10^\circ$ ) related to interplanar distances [10]. The VL $\alpha$  systems were further analyzed using the small angle x-ray scattering (SAXS) with Kratky compact Hecus system (Hecus X-ray system, Graz, Austria) equipped with a linear collimation system and x-ray tube Cu target ( $\lambda=1.54$  Å). The generator was implemented at a power of 2 kW (50 kV and 40 mA). The channel was calibrated at  $9.3 \times 10^{-4}$  Å<sup>-1</sup>, and the distance with the LC samples to the detector was set at 27.9 cm. The temperature was fixed at 23 °C  $\pm$  2 °C. The data for each sample was taken at 700 s.

**Differential scanning calorimetry.** The thermal behaviour of the VL $\alpha$  samples was carried out using DSC Q100. Firstly, the samples (5-10 mg) were precisely weighed in aluminium hermetic pans and then press-sealed. The empty pan was considered the point of reference. The N<sub>2</sub> flow rate employed was 50 mL/min in the temperature range of -20 °C to 60 °C of heating and cooling rate at 10 °C/min. The result recorded the second heating and cooling cycle.

**Rheological study.** The rheological behaviour of VL $\alpha$  samples was studied using a rotational strain rheometer PHYSICA MCR301 (Anton Par, Germany). To prevent sample slip, a cone-plate sensor (20 mm diameter, 1° angle) with a 1 mm gap and the sandblasted plate were used. Each batch was tested at least three times, and all measurements were taken from separate samples. The amplitude sweep was tested in the strain percentage of 0.001 to 100 at a constant frequency of 1 Hz. The frequency sweep was performed at 0.001 to 1 strain percentage

from LVR region at 0.1 to 1000 rad/s. The introduced liquid crystal's flow curve was then calculated using scanning (sweep) shear rate measurements with increasing shear rates from  $10^{-2}$  to  $10^3 \text{ s}^{-1}$

## Results and discussion

**Texture of Lamellar.** The macroscopic and microscopic analyses of VL $\alpha$  samples at different VCO content without and with 5% CB were performed after 24 h preparation using polarized light microscopy and the images are presented in Figure 1. All samples studied exhibited birefringent characteristics with a clear oily streak and maltese cross textures showing typical features of lamellar texture. This typical pattern is in line with the findings by Nor Ain et al. [11] and Salimin et. al. [12]. The results show that the lamellar texture is disturbed with an increase in oil content (Figure 1(d)) as indicated by a decrease in the intensity and density of the texture pattern. Based on the existence of a denser and uniform distribution pattern, the addition of 5% CB was found to have improved the lamellar texture stability of the M2 samples (Figure 1(e)). Whereas a different situation occurred to the M1 sample (Figure 1(b)) where the presence of CB slightly disturbed the stability of its lamellar texture. A more pronounced effect was observed at higher magnifications (20x) where more isotropic areas represented by a dark background had appeared explaining the disturbances in the lamellar texture of samples M1 (Figure 1(c)) compared to M2 (Figure 1(f)). However, a more accurate explanation with respect to lamellar texture stability can only be obtained through more in-depth studies such as characterization using SAXS, thermal and rheological profile studies.

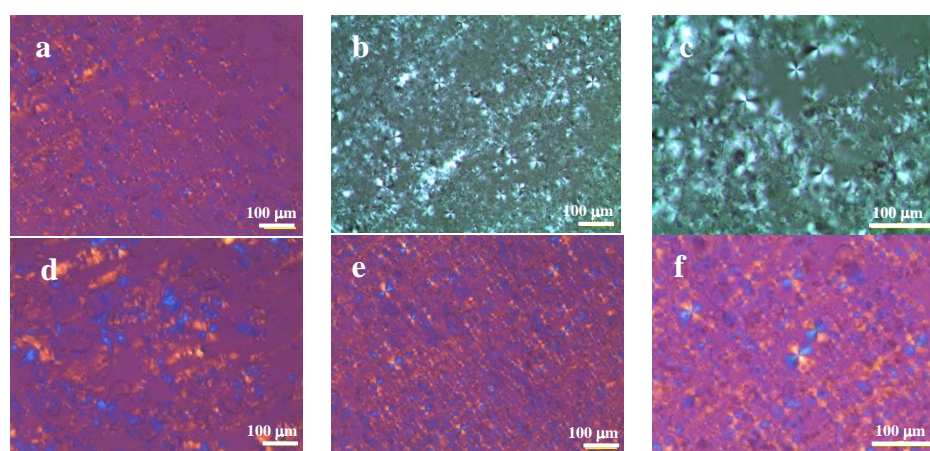


**Figure 1. Polarized light micrographs of VL $\alpha$  of a) M1, b) M1(5) at 10x magnification, c) M1(5) at 20x magnification, d) M2, e) M2(5) at 10x magnification and e) M2(5) at 20x magnification.**

**Measurement of physical properties.** Figure 2 shows that the L $\alpha$  phase may be distinguished by the characteristic ratio of the  $q$  values of the first and second ordered Bragg's peak equations, which is computed as follows:

$$d = 2\pi/q \quad (1)$$

Where ( $d$ ) is the interlayer spacing equation, and ( $q$ ) is the first order peak scattering vector. With increasing oil content along the oil dilution line, the first scattering peaks shift to higher  $q$  values, as measured by SAXS.

The SAXS analysis was limited to samples M1, M2, and M1 (5) to represent the whole VL $\alpha$  sample with a nearly similar PLM image pattern, and the spectrums are presented in Figure 2. The M<sub>S</sub>/H<sub>2</sub>O/VCO system displayed a typical lamellar liquid crystal with values of scattering vector  $q$  in the ratio of 1:2, demonstrating the L $\alpha$  phase characteristic of lamellar periodicity [13]. Based on the interlayer spacing ( $d$ ) listed in Table 1, the value of  $d$  increases slightly as the VCO content increases illustrating the weakness of the interaction between the hydrocarbon chains of surfactant. Meanwhile, based on a relatively consistent value of  $d$  it was found that the inclusion of CB did not affect the interaction of surfactant molecules between the lamellar layers, and the CB molecule was located between the surfactant hydrocarbon chains. In this study, SAXS analysis was performed only to confirm the existence of a lamellar phase without paying attention to the cross-sectional area per head group of surfactants.

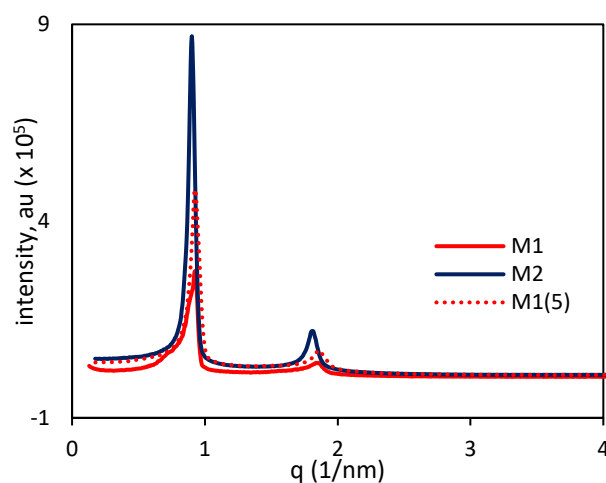


**Figure 2.** Small-angle X-ray scattering of VL $\alpha$  samples at 25°C. VL $\alpha$  of 3.5% VCO (M1), 6% VCO (M2) and 3.5% VCO with 5%CB (M1(5)).

**Table 1.** Compositions and interlayer spacing,  $d$  of VL $\alpha$  of samples from T85:T65/H<sub>2</sub>O/VCO systems.

Sample	VCO content (%)	Interlayer spacing, $d$ (nm)
M1	3.5	6.772
M2	6	6.913
M1(5)	3.5	6.716

**Thermal analysis.** DSC is used to study the thermal stability of the LC samples. Figure 3 illustrates the second heating and cooling curve of VL $\alpha$  systems based on DSC data. Melting peaks for samples M1, M2, and M2(5) were found at 20.25 °C, 21.50 °C, and 22.0 °C, respectively, throughout the heating cycle. These melting points are caused by the “melting” of the amount of VCO between the L $\alpha$  bilayers [14]. The phase transition from the crystalline to the lamellar mesophase is represented by these peaks [15]. The cooling cycle broad peak appears and the crystallization point has slightly shifted to a lower value due to the addition of VCO (0.76 °C to -2.49 °C) and CB (-2.49 to -4.49 °C) content. With this, it can be concluded that the VCO content and the presence of CB did slightly affect with the thermal stability of the VL $\alpha$ . A systematic DSC study of these samples also found that no phase transition occurred.

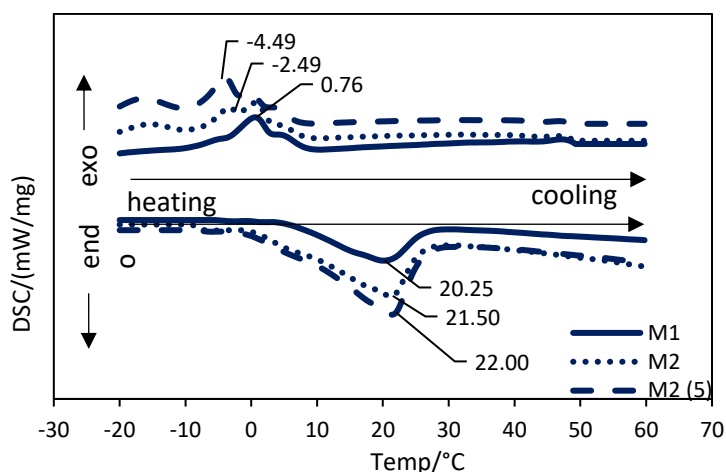


**Figure 3. DSC curve of the VL $\alpha$  of M1, M2 and M2(5) at heating and cooling rate of 10°C min<sup>-1</sup>.**

**Rheological study.** The rheological properties of the liquid crystal phase are linked to the structural arrangement of the surfactant aggregates and the many contact forces operating in the system. Rheological profiles have the potential to reveal a lot about the microstructure of liquid crystal phases. A rheological analysis investigation was performed on all of the formulated samples. Figure 4 depicts the amplitude sweep used to calculate the linear viscoelastic region (LVR), which will be used to identify the range within which the test can be conducted without damaging the sample's structure at the lowest strain value. All the rheological parameters are tabulated in Table 2. The sample in this study exhibits viscoelastic behaviour when  $G'$  is greater than  $G''$  and a much higher force is required to deform it within the LVR range of 0.01 to 1% strain. At 0.1% strain, the  $\tan \delta (= G''/G')$  value of the M1 sample is 4-times smaller than M2, indicating superior viscoelastic characteristics. Beyond the LVR regime, the  $G'$  and  $G''$  curves of all samples decreased consistently with  $G''$  being more dominant than  $G'$  explaining the creamy behaviour of the L $\alpha$  system [16]. This indicate that M1 is more stable than M2 in terms of rheological profile stability. An insignificant change in the value of  $\tan \delta$  indicates that the addition of CB to both samples had no discernible effect on the stability of the sample.

The frequency sweep measurement was used to investigate the sample's viscoelastic behaviour. The frequency sweep of all VL $\alpha$  samples analyzed are shown in Figure 5 and the frequency parameters are tabulated in Table 2. The elastic modulus  $G'$  is larger than viscoelastic modulus  $G''$  along the frequency investigated below the crucial point of angular frequency ( $\omega_c$ ) indicating that all samples behave more solidly.  $G'$  begins to drop after this point,  $G''$  slowly increase and becomes more dominating after crossover point, implying that the L $\alpha$  sample criteria shift to fluid-like behaviour at higher frequency strain [13]. According to Table 2, the  $\omega_c$  occurs at 22.1 rad/s and 41.8 rad/s for M1 and M2, respectively. Although M2 had a nearly two-fold higher value of  $\omega_c$  than M1, its evolutionary pattern of  $G'$  was practically frequency-dependent, especially around the  $\omega_c$ , and the value of  $\tan \delta$  was close to 1, indicating that the pseudoplastic properties of M2 was weaker than M1. The similar result was shown for 5% CB addition in both samples individually where no significant change occurred in the rheological profile. Aside from that, elastic characteristics may be compared using the lowest relaxation time ( $\tau_{\min}$ ) derived from  $1/\omega_{\text{crossover point}}$ . M1 sample has the lowest  $\tau_{\min}$  ( $\omega_{\text{crossover point}} = 78.8$

rad/s), which is 0.013 s, compared to M2 and M2(5), which have 0.024 s, indicating that the M1 sample has stronger pseudoplastic characteristics. This behaviour shows that the inner structure of the  $L\alpha$  phases is compatible and the long-term stability of the dispersion.

The flow curve in Figure 6 and flow curve parameters in Table 2 show that the rate of viscosity reduction (power law index) of most samples is not consistent along the shear rate studied. The power-law index describes four different patterns of viscosity reduction rate ranges, namely shear rates  $<1 \text{ s}^{-1}$ ,  $1 - 10 \text{ s}^{-1}$ ,  $10 - 100 \text{ s}^{-1}$ , and  $100 - 1000 \text{ s}^{-1}$ . A power law can describe these flow curves and Curreau shear-thinning models of  $\eta = k\gamma^{(n-1)}$  where  $\eta$  is the viscosity,  $\gamma$  the shear rate, and  $-(n-1)$  is the power-law index [17]. The exponent of  $-(n-1)$  close to -1 shows the shear thinning behaviour meanwhile the value close and above to 0 shows the shear thickening behaviour. The  $-(n-1)$  value represents the arrangement of  $L\alpha$  structure, whether parallel and continuous or irregular and random organization [18-19].

At low shear rates ( $<1 \text{ s}^{-1}$ ), the power-law index of all samples was around -1 (Table 2) regardless of VCO content, indicating shear-thinning behaviour of plastic materials [1]. Based on the drastic increase in the value of  $\tan \delta$  and the relative decrease in the viscosity ( $\eta_0$ ), the increase in VCO (M2) was found to cause the pseudoplastic properties to weaken. However, the shear thinning behaviour of samples in the presence of high VCO content increased especially at high shear rate ( $-10$  to  $1000 \text{ s}$ ). This may be due to the slippery nature of the VCO which makes it less resistant to shear. Similar phenomenon has occurred for the addition of 5% CB, where it improves the shear thinning behaviour of the samples at a higher shear rate range of  $100-1000 \text{ s}^{-1}$  especially for M1. The power law index increased almost 3-fold due to the presence of hydrophobic molecules of CB indicating an increase in the strength and durability of the  $VL\alpha$  network against shear [1]. A steady decrease in  $\eta_0$  with the addition of CB occurred regardless of VCO content. The surfactant molecules freely aggregate in the  $VL\alpha$  system as the CB added in  $VL\alpha$  system and sliding occurs in any potential  $L\alpha$  direction, with no driving force for the structure to relax back to its previous form [20].

Based on this rheological study, the shear thinning properties shown by the formulation of Ms/  $\text{H}_2\text{O}$ /VCO has great potential to be applied in the pharmaceutical, cosmetics and microfluidics industries. The incorporation of 5% CB particularly in  $VL\alpha$  samples with an oil content of 3.5% has the potential to be used for the treatment of AD.

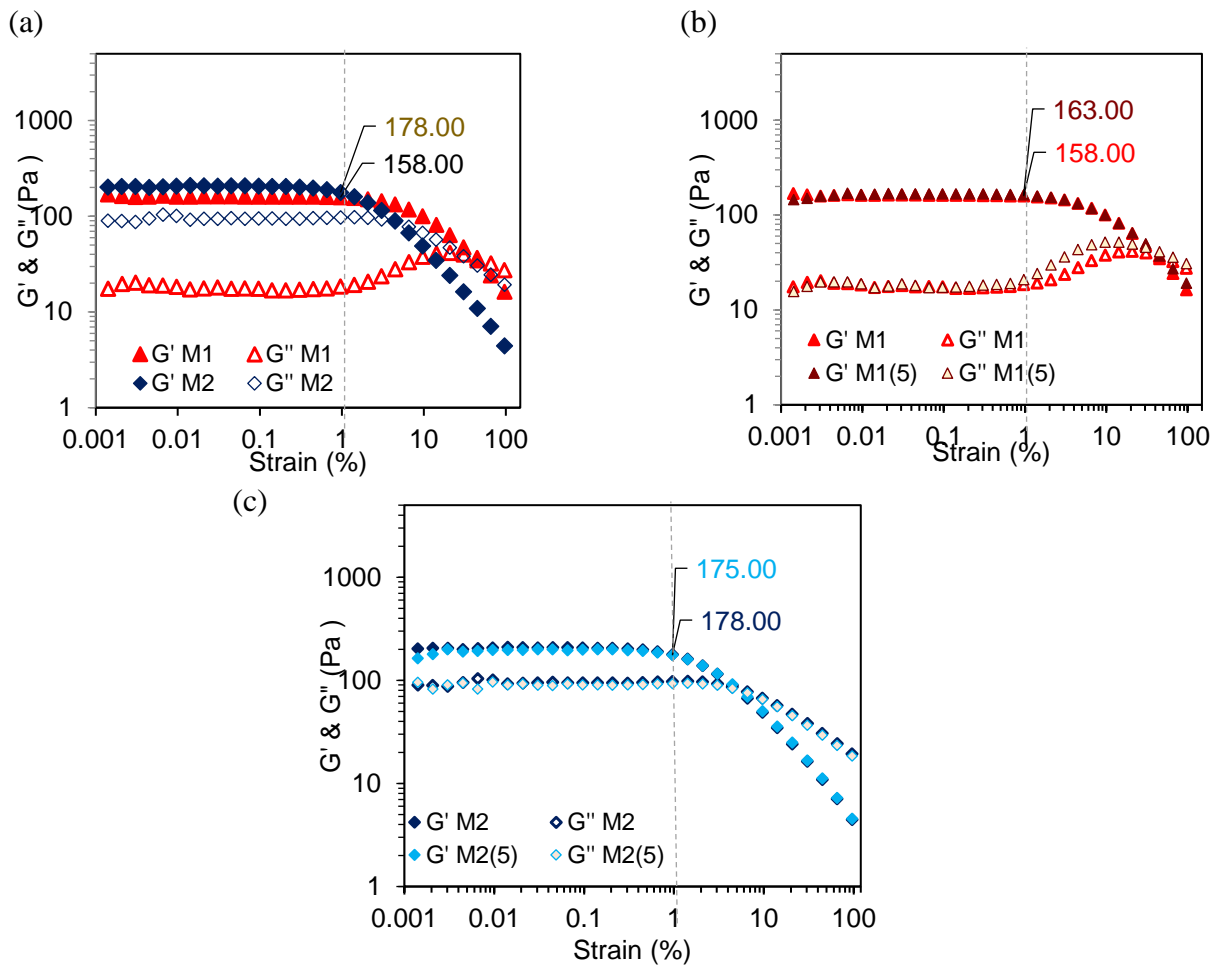


**Figure 4. Amplitude sweep of VL $\alpha$  samples at a) different VCO content (3.5% and 6%) b) 3.5% VCO without and with 5%CB, and c) 6% VCO without and with 5%CB.**

**Table 2. Frequency and flow curve parameters of VL $\alpha$  samples.**

Sample	VCO content (%)	$\eta_0$ (Pa.s)	Tan $\delta$	$\omega_c$ (rad/s)	$\omega_{\text{crossover point}}$ (rad/s)	-(n-1)			
						<1s <sup>-1</sup>	1-10s <sup>-1</sup>	10-100s <sup>-1</sup>	100-1000s <sup>-1</sup>
M1	3.5	365	0.109	22.1	78.8	-0.710	-0.596	-0.410	-0.234
M2	6	164	0.457	41.8	41.8	-0.716	-0.528	-0.534	-0.489
M1(5)	3.5	316	0.104	30.5	45.6	-0.700	-0.559	-0.210	-0.652
M2(5)	6	145	0.456	6.57	75.3	-0.704	-0.513	-0.532	-0.510

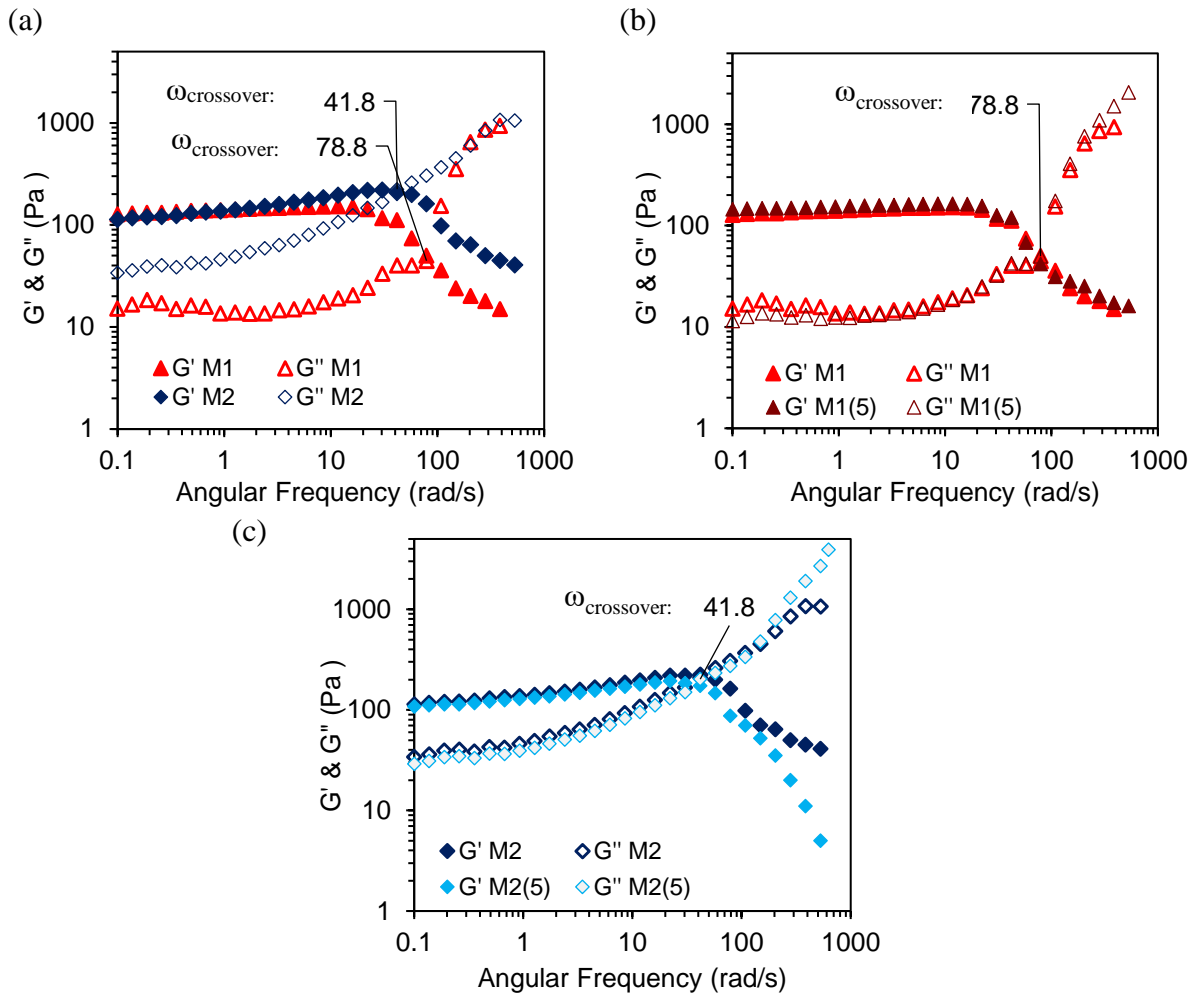


**Figure 5. Frequency sweep of VLa samples at a) different VCO content (3.5% and 6%) b) 3.5% VCO without and with 5%CB, and c) 6% VCO without and with 5%CB**

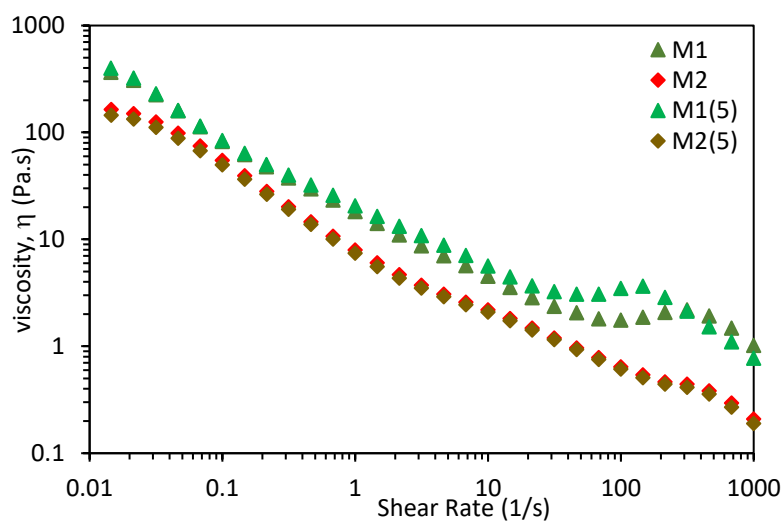


**Figure 6. Flow curve of VLa samples of M1, M2, M1(5) and M2(5).**

## Conclusion

This study revealed that Ms/H<sub>2</sub>O/VCO exhibits lamellar liquid crystal phases at a constant Ms/H<sub>2</sub>O ratio of 0.69:0.31. The VCO content was discovered to affect the lamellar texture and the rheological profile without having a substantial impact on thermal stability. Both of these samples, particularly sample M1, were able to handle the presence of CB without causing considerable disturbance to the lamellar structure. As a result, sample M1 is the most desired formulation since it has a consistent shear-thinning pattern and greater elastic characteristics.

## Acknowledgement

This research has been carried out under Fundamental Research Grants Scheme (FRGS/1/2019-0004-102-02) provided by the Ministry of Education of Malaysia. The authors would like to extend their gratitude to Universiti Pendidikan Sultan Idris (UPSI) that helped manage the grants.

## Author contributions

All authors contributed toward data analysis, drafting and critically revising the paper and agree to be accountable for all aspects of the work.

## Disclosure of conflict of interest

The authors have no disclosures to declare.

## Compliance with ethical standards

The work is compliant with ethical standards.

## References

- [1] Joshua, B., Matthew, J., Thomas, M., Liliana, D. C., Anna, S., Toby, D.M. & Rico, F. T. (2018). Structural and rheological changes of lamellar liquid crystals as a result of compositional changes and added silica nanoparticles. *Phys. Chem. (Royal Society of Chemistry)*.20(24) 16592-16603.
- [2] Cong, Z., Lin, B., Li, W., Niu, J. & Yan, F. (2017). Lamellar liquid-crystalline system with tunable iridescent color by ionic surfactants. *Langmuir*. 33(28) 7147–7151.
- [3] Terescenco, A. D., Picard, C., Grisel, M., & Savary, G. (2017). Influence of the emollient structure on the properties of cosmetic emulsion containing lamellar liquid crystals. *Colloids and Surfaces A: Physicochem. Eng. Aspects*. 536 10-19

- [4] Suryani, S., Sariyani, S., Earnestly, F., Marganof, M., Rahmawati, R., Sevindraajuta, S., Indra Mahlia, T. M., & Fudholi, A. (2020). A comparative study of virgin coconut oil, coconut oil and palm oil in terms of their active ingredients. *Processes*. 8(4) 1–11.
- [5] Varma, S. R., Sivaprakasam, T. O., Arumugam, I., Dilip, N., Raghuraman, M., Pavan, K. B., Rafiq, M., & Paramesh, R. (2019). In vitro anti-inflammatory and skin protective properties of virgin coconut oil. *J. Trad. Comp. Med.* 9(1) 5–14.
- [6] Fishbein, A. B., Silverberg, J. I., Wilson, E. J., & Ong, P. Y. (2020). Update on atopic dermatitis: diagnosis, severity assessment, and treatment selection. *J. Allerg. Clin. Immunol.* 8(1) 91-101.
- [7] Monte, B., S. F. M., Santos, J. S., Feltes, M. M. C., Dors, G., Licodiedoff, S., Lerin, L. A., de Oliveira, D., Ninow, J. L., & Furigo, A. (2015). Optimization of diacylglycerol production by glycerolysis of fish oil catalyzed by lipozyme TL IM with tween 65. *Bioprocess. Biosystems Eng.* 38(12) 2379–2388.
- [8] Huang, Y., & Gui, S. (2018). Factor affecting the structure of lyotropic liquid crystals and the correlation between structure and drug diffusion. *RSC Adv.* 8(13) 6978-6987.
- [9] Dalila, ARN (2012) Phase Diagrams of Tweens Series (21, 65, 81, 85)/Water/Virgin Coconut Oil and Mixed Tweens/Water/Virgin Coconut Oil Systems. (*B. Edu.S. Thesis*, Universiti Pendidikan Sultan Idris, Perak, Malaysia) pp. 22-23.
- [10] Dante, M. de C. L., Borgheti-Cardoso, L. N., Fantini, M. C. de A., Praça, F. S. G., Medina, W. S. G., Pierre, M. B. R., & Lara, M. G. (2018). Liquid crystalline systems based on glyceryl monooleate and penetration enhancers for skin delivery of celecoxib: characterization, in vitro drug release, and in vivo studies. *J. Pharmaceut Sci.* 107(3) 870–878.
- [11] Nor Ain M. A, Mahamod, W. R. W., Bakar, N. A., Hashim, N., Isnolamran, N. H. & Shamsudin, S. A. (2021). The effect of virgin coconut oil content on the rheological profile of virgin coconut oil-based lamellar liquid crystal of mixed tween 80: brij 30 system. *Malaysian Journal of Microscopy*. 17(2) 195-207.
- [12] Salimin, N. R., Mahamod, W. R. W., Bakar, N. A., Azziz, S. S. S. A., Sharif, A. M., Pauzan, N. A., & Hashim, N. (2019). Characterisation of virgin coconut oil based lamellar liquid crystal incorporated with lycopene. *J. of Adv Research in Dynamical & Control Systems*. 11(06) 1852-1858.
- [13] Li, H., Dang, L., Yang, S., Li, J., & Wei, H. (2016). The study of phase behavior and rheological properties of lyotropic liquid crystals in the LAS/AES/H<sub>2</sub>O system. *Colld. Surf. A: Physicochem. Eng. Asp.* 495(5) 221–228.
- [14] Li, Y., Dong, C., Cun, D., Liu, J., Xiang, R., & Fang, L. (2016). Lamellar liquid crystal improves the skin retention of 3-O-ethyl-ascorbic acid and potassium 4-methoxysalicylate in vitro and in vivo for topical preparation. *AAPS Pharm. Sci. Tech.* 17(3) 767–777.
- [15] Selivanova, N. M., Konov, A. B., Romanova, K. A., Gubaidullin, A. T., & Galyametdinov, Y. G. (2015). Soft matter lyotropic  $\alpha$ -containing lamellar liquid crystals: phase behaviour, thermal and structural properties. *Soft Matter*. 11 (39) 7809-7816.

[16] Mislan, A. A., Foong, J. L. N., Saharin, S. M., & Zahid, N. I. (2019). Rheological behaviour of thermotropic and lyotropic liquid crystalline phases of guerbet branched chain glycolipids. *Fluid Phase Equilibria*. 502 1-12.

[17] P. Kumar, U. N. Maiti, K. E. Lee, and S. O. Kim. (2014). Rheological properties of graphene oxide liquid crystal. *Carbon*. 80(1),453–461.

[18] Z. Li, X. Zhao, and Z. Wang. (2017). Rheological properties of lyotropic liquid crystals encapsulating curcumin. *J. Dispers. Sci. Technol*. 38(1) 132-138.

[19] S.A.M. Silva, R. Lacerda, J. Bernegossi, M. Chorilli, and G.R, Leonardi. (2016). Rheological characterization and safety evaluation of non-ionic lamellar liquid crystalline systems containing retinyl palmitate. *J. Biomedic Nanotech*. 12(10) 394-403.

[20] Fan, J., Liu, F., & Wang, Z. (2016). Shear rheology and in-vitro release kinetic study of apigenin from lyotropic liquid crystal. *Int. J. Pharm*. 497(1-2) 248-254